JOURNAL OF CATALYSIS 139, 652–663 (1993)

Catalytic Partial Oxidation of Methane over Ba–Pb, Ba–Bi, and Ba–Sn Perovskites

DHAMMIKE DISSANAYAKE, KARL C. C. KHARAS,[1] JACK H. LUNSFORD, AND MICHAEL P. ROSYNEK[2]

Department of Chemistry, Texas A & M University, College Station, Texas 77843

Received July 1, 1992; revised September 16, 1992

Catalytic behaviors of the stoichiometric perovskites $BaPbO_3$, $BaBiO_3$, and $BaSnO_3$, and of corresponding materials containing excess Ba, have been investigated for the oxidative coupling of methane. The Ba–Pb and Ba–Bi perovskites are more active and produce substantially higher C_2 product yields (12–15%) at 800°C than does the Ba–Sn material (4%). XRD analyses of the used catalysts indicate that $BaPbO_3$ and $BaBiO_3$ undergo extensive bulk decomposition under CH_4/O_2 reaction conditions, forming $BaCO_3$ and BaO_2 phases, together with either PbO_x, or Bi_2O_3. XPS characterization reveals that the surfaces of both materials become enriched in Ba as a result of their bulk decompositions. $BaSnO_3$, by contrast, does not undergo significant changes in either its bulk or surface compositions as a result of the oxidation reaction. A significant portion of the surface Ba on these materials during reaction exists as $BaCO_3$, which is generated from the CO_2 reaction product and which is partially converted into the active BaO_2 phase by reaction with O_2.

INTRODUCTION

The partial catalytic oxidation of methane to produce higher hydrocarbons has been an active field of research for the last several years, for both practical and fundamental reasons (*1*, *2*). Substantial deposits of natural gas, composed primarily of methane, have been discovered recently; however, most of these resources are located in remote areas, and the cost and potential hazards of transport have prevented their large scale introduction to industrial markets (*3*). Therefore, it is desirable to develop a process for converting the methane component of natural gas into less volatile and more valuable products prior to shipment from the production site. Oxidative coupling of methane to C_{2+} products is a potential route for such natural gas conversion; however, the achievement of an oxidative activation of one relatively strong C–H bond of methane under conditions where both complete oxidation of the methane and subsequent oxidation of the more reactive higher hydrocarbon products are minimized presents a challenging chemical problem.

Many metal oxides, particularly basic oxides such as rare earth sesquioxides, alkaline earth oxides, and alkali metal-containing metal oxides, are active and selective catalysts for the oxidative coupling of methane (*1*). These different types of metal oxides may activate methane via differing types of surface oxygen species; however, only a few fundamental studies regarding the oxygen species responsible for the catalytic activation of methane over metal oxides have been carried out. Ito and Lunsford proposed that $[Li^+O^-]$ centers are responsible for methane activation over Li-promoted MgO (*4*). The methyl radicals produced by these centers then undergo coupling in the gas phase to produce ethane. Methyl radicals emanated into the gas phase may also be involved in various autocatalytic homogeneous reactions that may con-

[1] Present address: Allied-Signal Corp., Chicago, IL.
[2] To whom correspondence should be addressed.

0021-9517/93 $5.00

vert additional oxygen and methane. Otsuka *et al.* have demonstrated that ethane, *n*-butane, and *n*-hexane are the primary coupling products of methane, ethane, and propane, respectively, over Na_2O_2, where the active oxygen species are peroxide ions (*5*). Moreover, the reactions were carried out at significantly lower temperatures (<400°C) than those typically required (≥700°C) for oxidative coupling of methane over most metal oxides. Although these reactions are not catalytic, they provide useful information regarding the nature of surface oxygen sites that are capable of activating methane. In addition to Na_2O_2, other stable peroxides, such as SrO_2 and BaO_2, have also been reported to activate methane via the peroxide species (*6*). Otsuka and Jinno suggested that diatomic oxygen species such as O_2^{2-}, O_2^- or chemisorbed O_2 are responsible for the activation of methane over Sm_2O_3 (*7*).

X-ray photoelectron spectroscopy (XPS) has been a particularly effective technique for establishing the nature of the active phases in both supported and unsupported partial oxidation catalysts (*8–10*). In an XPS study of Li/MgO, Stair and co-workers reported that the active phase for oxidative coupling of methane is $[Li^+O^-]$ (*8*). They obtained a correlation between the intensity of the O 1*s* photoelectron line centered at 533.0 eV, which was assigned to surface oxygen in the $[Li^+O^-]$ centers, and the activity for methane conversion. In a more recent publication by the same group, it is reported that the active centers in Na-doped CaO consist of Na species associated with CaO (*9*). Deactivation of this catalyst was attributed to the formation of $CaCO_3$. Recently, Yamashita *et al.* examined a series of barium–lanthanum mixed oxides and determined that the active species responsible for methane activation over these materials is O_2^{2-} (*10*). They further suggest that these peroxide species may decompose into O_2^- or O^- at the high temperatures where these oxides are capable of activating methane. They concluded that, in order for such decomposition to occur, the BaO_2 must be highly dispersed on the Ln_2O_3 support.

Rao *et al.* have also employed XPS to characterize peroxide-like species in mixed metal oxides (*11*). The presence of such oxygen species has been correlated with the metallicity and superconductivity of these materials. The oxygen species present in perovskite-structure mixed metal oxides have been studied by Ganguly and Hegde (*12*). Using XPS, they have delineated the O^{2-} and O_2^{2-} species that are present in materials such as PbO_2, $BaPbO_3$, $BaBiO_3$ and $SrPbO_3$. Lunsford and Kharas have investigated the catalytic properties of these perovskites and correlated their catalytic properties to the presence of peroxidic oxygen (*13, 14*). The metallic (and super conducting) $BaPbO_3$ and the semiconducting $BaBiO_3$ which are both formulated as $A^{2+}B^{2+}[O_2^{2-}]O^{2-}$ perovskites, were found to be active oxidation catalysts and to be selective for hydrocarbon product formation. A closely related material, $BaSnO_3$, which is formulated as an $A^{2+}B^{4+}[O^{2-}]$ perovskite, was also found to be an active oxidation catalyst, but one which is selective for complete, rather than partial, oxidation.

EXPERIMENTAL

The reagents $Bi(NO_3)_3$ (99.9%), $Pb(NO_3)_2$ (99.5%), and $Ba(NO_3)_2$ (99%) were purchased from Aldrich Chemical Co. The perovskites $BaBiO_3$ and $BaPbO_3$ were synthesized using a previously published technique (*15*). An aqueous solution containing appropriate concentrations of barium and bismuth or lead nitrates was evaporated to dryness, and the resulting solid was heated to 800°C for 12 h. Ba–Pb and Ba–Bi compounds containing a 100% excess of Ba were also synthesized by this method. The Ba–Pb perovskite was also synthesized via the nitrate solid solution method (*15*). Crystalline phases of the synthesized compounds were identified by X-ray powder diffraction (XRD) analyses. The $BaSnO_3$ perovskite was purchased from Johnson Matthey. A sample of $BaSnO_3$containing a 100% excess

TABLE 1

BET-N_2 Surface Areas of Catalysts (m^2/g)

Condition	$BaPbO_3$	$BaBiO_3$	$BaSnO_3$
Fresh	0.6	0.2	0.8
Used[a]	0.7	0.2	0.9

[a] 10 h at 800°C; $CH_4 : O_2 = 4 : 1$.

of Ba was prepared by impregnating the original perovskite with an appropriate amount of $Ba(NO_3)_2$, followed by calcination for 12 h at 800°C. The reactant gases, viz., ultra-high purity (99.9%) CH_4 and O_2 from Matheson and high purity (99.995%) He from Airco, were further purified by passage through a 5A molecular sieve column at 25°C prior to use. The catalytic reactors, having an internal diameter of 5.0 mm, were fabricated from high purity tubular alumina obtained from Omega. Such a reactor, when filled only with quartz chips and exposed to the reaction mixture at typical reaction temperatures (800°C), gave no appreciable CH_4 conversion. In a typical experiment, 500 mg of 20–40 mesh catalyst particles were loaded into the reactor and pretreated in flowing oxygen for 1 h at 800°C. The feed was then switched to the reaction mixture of CH_4 (16 ml/min), O_2 (4 ml/min), and He (30 ml/min).

The reactor effluent was analyzed by gas chromatography, using a TCD detector. H_2O, CO_2, C_2H_6, and C_2H_4 were separated from CH_4, CO, and O_2 on a Chromosorb 107 column. The latter three components were separately analyzed using a molecular sieve 13X column. Catalytic experiments were performed both by changing the reaction temperature at constant CH_4/O_2 reactant ratio and by varying the CH_4/O_2 ratio at constant temperature. Experiments were also done for extended reaction times (25 h) at a fixed temperature (800°C) and a constant CH_4/O_2 ratio. BET-N_2 surface areas of the three catalysts were measured before and after the catalytic experiments, and are summarized in Table 1. The original $BaSnO_3$, as purchased from Johnson Matthey, had a relatively large surface area (2.5 m^2/g) compared to those of the synthesized $BaBiO_3$ and $BaPbO_3$. In order to more accurately compare the catalytic activity and selectivity of this material to those of $BaPbO_3$ and $BaBiO_3$, the $BaSnO_3$ use in these experiments was sintered at 1000°C to decrease its surface area to a value comparable to those of the Ba–Pb and Ba–Bi perovskites.

X-Ray photoelectron spectra (XPS) were acquired on a Perkin–Elmer Model 5500 Multi-Technique Surface Analysis System equipped with a dual Mg–Zr anode. All measured binding energies were adjusted with respect to the C 1*s* peak at 284.6 eV due to adventitious carbon. The catalyst samples were pressed into wafers and were mounted on a Pt foil-covered ceramic sample holder for XPS analysis. In order to ensure identical catalyst surface conditions as those resulting from the catalytic reaction experiments, these samples were treated prior to XPS analysis in a fused quartz reactor in flowing O_2 and in the same flow of CH_4, O_2, and He as those employed for the reaction studies. (Blank experiments confirmed that the Pt foil contributed negligibly to the total CH_4 conversion under the reaction conditions employed.) The samples were then transported under He or O_2 in an O-ring-sealed transfer vessel to the XPS introduction chamber, without exposure to the atmosphere. The design of the reactor assembly avoided the necessity of handling the samples in a glove box. The base pressure of the XPS analysis chamber was 5×10^{-10} Torr. Spectra were recorded for samples both after O_2 treatment and after exposure to the CH_4/O_2/He reaction mixture for various lengths of time. In a typical XPS data acquisition, a pass energy of 29.35 eV, step increment of 0.125 eV, and Mg anode power of 300 Watts provided an adequate combination of resolution and data collection time. The photo electrons were collected at an angle of 45° to the sample surface for 7 min in each of the spectral regions: O 1*s*, C 1*s*, Ba 3*d*, Pb 4*f*, Bi 4*f*, and Sn 3*d*. Near-surface

compositions were calculated from peak areas in the latter regions, using appropriate sensitivity factors for each line.

X-ray powder diffraction (XRD) analyses were performed both before and after exposing the samples to the reactant gas mixture, using a Rigaku Model RU200 diffractometer. Deuterium exchange experiments were carried out in order to verify that the pretreated catalysts were free of surface OH groups, whose O 1*s* peak interferes with that of the peroxide ion. In these experiments, D_2 was allowed to equilibrate with the catalyst sample at 500–600°C for 2 h in a sealed quartz vessel, after which mass spectra of the equilibrated gas phase were obtained. These experiments provided the necessary information to estimate the surface coverage of OH groups.

RESULTS AND DISCUSSION

Catalytic Behaviors

In order to obtain additional information about the nature of sites that are involved in the activation of methane on metal oxide surfaces, $BaPbO_3$ and $BaBiO_3$ were selected for study because both have been reported to contain lattice O_2^{2-} species due to oxygen valance fluctuation (*12*), whereas the perovskite $BaSnO_3$ does not contain O_2^{2-} species (*14*). As shown in Figs. 1 to 4, $BaPbO_3$ and $BaBiO_3$ are more selective catalysts than is $BaSnO_3$ for the oxidative coupling of methane. Data are also included in these figures for Ba-rich samples of each perovskite. The twofold excess of Ba was introduced in each case by the addition of an appropriate excess of $Ba(NO_3)_2$ during the preparation described previously. As confirmed by XRD analyses, this procedure did not produce stoichiometrically distinct compounds, but merely stoichiometric Ba–Pb, Ba–Bi, and Ba–Sn perovskites containing a separate BaO_x phase.

After initial changes during the first two hours of reaction, all of the catalysts except $BaBiO_3$ maintained a constant activity over the time period investigated. Under oxygen-limited conditions at 800°C (Fig. 1), methane

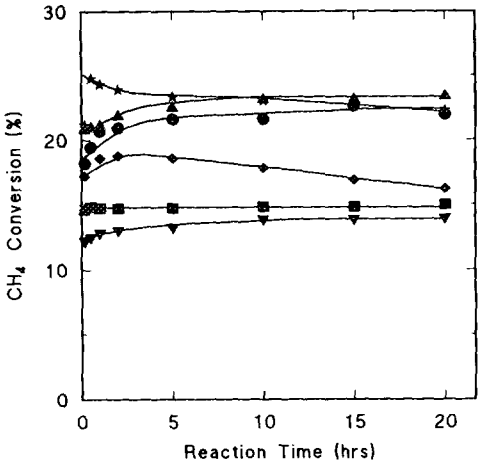

FIG. 1. Variation of methane conversion with reaction time. ●, $BaPbO_3$; ▲, $BaPbO_3$ + excess Ba as BaO_2; ◆, $BaBiO_3$; ▼, $BaBiO_3$ + excess Ba as BaO_2; ■, $BaSnO_3$; ★, $BaSnO_3$ + excess Ba as BaO_2. (T = 800°C; CH_4O_2/He = 16/4/30 ml/min.)

conversions over $BaPbO_3$ and $BaBiO_3$ reached 22% and 16%, respectively, with C_2 selectivities exceeding 60% (Fig. 2). Methane conversion and C_2 selectivity over $BaSnO_3$, by contrast, were only 15 and 30%, respectively. These values were markedly

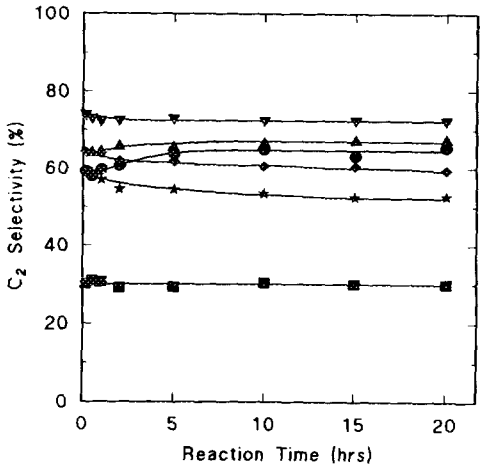

FIG. 2. Variation of C_2 product selectivity with reaction time. ●, $BaPbO_3$; ▲, $BaPbO_3$ + excess Ba as BaO_2; ◆, $BaBiO_3$; ▼, $BaBiO_3$ + excess Ba as BaO_2; ■, $BaSnO_3$; ★, $BaSnO_3$ + excess Ba as BaO_2. (T = 800°C; CH_4/O_2/He = 16/4/30 ml/min.)

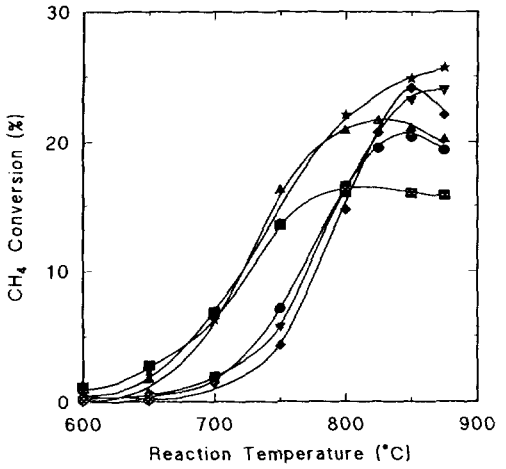

FIG. 3. Variation of methane conversion with reaction temperature. ●, $BaPbO_3$; ▲, $BaPbO_3$ + excess Ba as BaO_2; ◆, $BaBiO_3$; ▼, $BaBiO_3$ + excess Ba as BaO_2; ■, $BaSnO_3$; ★, $BaSnO_3$ + excess Ba as BaO_2. (CH_4/O_2/He = 16/4/30 ml/min.)

higher (22 and 53%, respectively), however, when an excess of Ba was present on the $BaSnO_3$. When the $CH_4:O_2$ reactant ratio was increased from 4:1 to 10:1, the C_2 selectivity over $BaPbO_3$ increased from 60 to 70%, with an accompanying decrease in CH_4 conversion from 17 to 8%, while over $BaBiO_3$, the selectivity increased from 65 to 72%, and the conversion decreased from 13 to 4%. When compared under non-oxygen-limited conditions (Figs. 3 and 4), all three samples containing excess Ba consistently displayed higher methane conversions and selectivities to C_2 compounds than did their stoichiometric counterparts throughout most of the temperature range investigated. The effect was particularly pronounced for $BaSnO_3$. At temperatures $\geq$ 800°C, when the reaction became oxygen-limited, the activities and selectivities over the stoichiometric $BaPbO_3$ and $BaBiO_3$ perovskite phases approached those over the samples containing excess Ba. Although methane conversion levels over $BaSnO_3$ are comparable to those over the Ba–Pb and Ba–Bi compounds, this material displayed comparatively low C_2 selectivity. O_2 conversion over the Ba–Pb and Ba–Sn materials reached 100% in the temperature range 750–800°C, and for the Ba–Bi materials in the temperature range 800–825°C. This could be due to the somewhat lower surface area of the Ba–Bi compound compared to those of Ba–Pb and Ba–Sn (Table 1).

It is significant that the methane conversion activity over all of the catalysts, except the two $BaSnO_3$ materials, increased during the first few hours of reaction (Fig. 1). It is also noteworthy that this increase was more pronounced for the stoichiometric Ba : Pb and Ba : Bi perovskites than for the samples containing excess Ba. Moreover, XRD analyses confirmed that, particularly for $BaPbO_3$, the original perovskite phases underwent extensive transformation following exposure to the reaction mixture, as summarized in Table 2. Although the activity increased during the first few hours of the reaction, the C_2 selectivity did not show a corresponding increase for the two Ba–Bi compounds. In the case of $BaSnO_3$, by contrast, neither the activity nor the C_2 selectivity varied from their initial values throughout the 25-h reaction period. The increase in

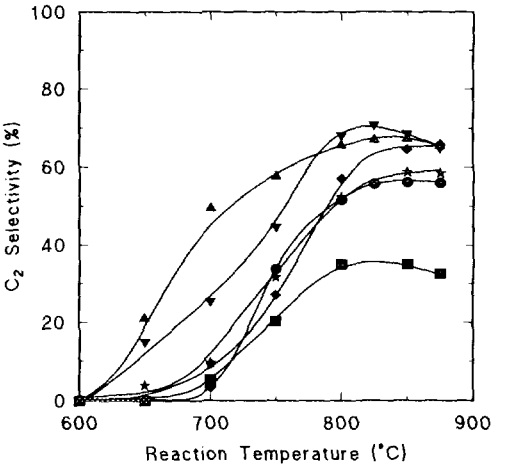

FIG. 4. Variation of C_2 product selectivity with reaction temperature. ●, $BaPbO_3$; ▲, $BaPbO_3$ + excess Ba as BaO_2; ◆, $BaBiO_3$; ▼, $BaBiO_3$ + excess Ba as BaO_2; ■, $BaSnO_3$; ★, $BaSnO_3$ + excess Ba as BaO_2. (CH_4/O_2/He = 16/4/30 ml/min.)

TABLE 2

Bulk Catalyst Phases Observed by XRD

Fresh	Used[a]	
$BaPbO_3$	$BaPbO_3$	(20%)
	$BaCO_3$	(50%)
	BaO_2	(15%)
	PbO_x	(15%)
$BaBiO_3$	$BaBiO_3$	(85%)
	$BaCO_3$	(5%)
	BaO_2	(5%)
	Bi_2O_3	(5%)
$BaSnO_3$	$BaSnO_3$	

[a] 10 h at 800°C; $CH_4:O_2 = 4:1$.

catalytic activity for the Ba–Pb and Ba–Bi catalysts during the first 2 h of reaction, together with the accompanying phase transformations of these materials, suggest that the number or the activity of the existing active sites over these materials increases as the original perovskite phase decomposes. It is possible, therefore, that the O_2^{2-} species in the original monophasic oxides may not play a significant role in determining their activity and C_2 selectivity. The necessary involvement of a surface lattice oxygen species, however, in the catalytic sites was confirmed by exposing an oxygen-pretreated $BaPbO_3$ sample to pure methane at 700°C and observing ethane, ethylene, and water products in the gas phase. Carbon dioxide was not observed in the gas phase, but this is likely due to its absorption by the catalyst.

XPS Characterization

In order to investigate the nature of the surface sites involved in methane oxidation, the catalysts were examined further using XPS. Figure 5 presents spectra in the Sn 3*d*, Bi 4*f*, and Pb 4*f* regions for both the fresh catalysts and for ones that had been exposed to a $4:1$ $CH_4:O_2$ reaction mixture for 10 h at 800°C. The Sn 3*d* spectrum of $BaSnO_3$ was unchanged following exposure to the reaction mixture. Spectra for both $BaBiO_3$ and $BaPbO_3$, however, indicated the formation of new species, having Bi and Pb 4*f* binding energies higher than those in the original perovskites. The effect is particularly noticeable in the case of $BaPbO_3$, where the appearance of a new lead species in the near-surface region is apparent in the Pb 4*f* spectrum of the used catalyst. These XPS results are consistent with the previously discussed XRD data for the used catalysts (Table 2), which indicated the formation of bulk bismuth and lead oxides, following exposure to the $CH_4:O_2$ reaction mixture. These changes in the Bi and Pb surface environments of $BaBiO_3$ and $BaPbO_3$, resulting from use as catalysts for methane oxidation, were accompanied by an enrichment of Ba in the near-surface regions, as shown in Table 3, where the near-

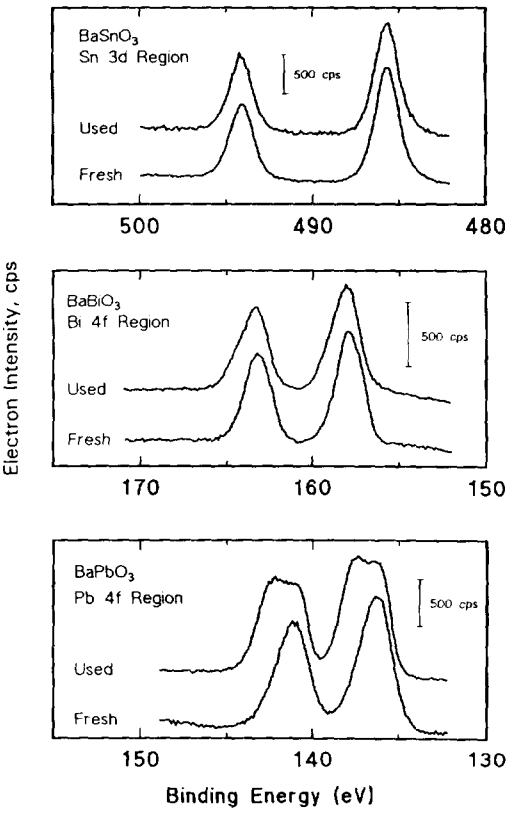

FIG. 5. XPS spectra in metal regions for fresh and used ($CH_4:O_2 = 4:1$ for 10 h at 800°C) perovskite catalysts.

TABLE 3

Surface Compositions of Catalysts Determined by XPS

Catalyst	Surface Composition (atomic%)								
	O	C[a]	Ba	Pb	Bi	Sn	Ba/Pb	Ba/Bi	Ba/Sn
$BaPbO_3$ (fresh)	57	0	21	22			0.9		
$BaPbO_3$ (used)[b]	57	25	12	6			2.2		
$BaPbO_3$ + excess Ba (fresh)	60	0	33	7			4.5		
$BaPbO_3$ + excess Ba (used)[b]	59	25	13	3			4.7		
$BaBiO_3$ (fresh)	56	0	22		22			1.0	
$BaBiO_3$ (used)[a]	50	20	21		9			2.3	
$BaBiO_3$ + excess Ba (fresh)	66	0	21		13			1.6	
$BaBiO_3$ + excess Ba (used)[b]	51	22	21		6			3.5	
$BaSnO_3$ (fresh)	54	0	24			22			1.1
$BaSnO_3$ (used)[b]	44	9	24			23			1.1
$BaSnO_3$ + excess Ba (fresh)	63	0	26			11			2.4
$BaSnO_3$ + excess Ba (used)[b]	63	18	19			0			—

[a] Carbon in CO_3^{2-} species only; does not include adventitious carbon.
[b] 10 h at 800°C; $CH_4 : O_2 = 4 : 1$.

surface compositions of the fresh and used catalysts are summarized. (The carbon contents listed are due only to surface carbonate species, and do not include contributions from adventitious surface carbon.) It was not possible to confirm the formation of a new barium species, if any, by XPS because the binding energy of the Ba 3*d* photoelectron line at 779.1 ± 0.1 eV is virtually unaffected by changes in the Ba chemical environment. The used $BaSnO_3$ exhibited essentially no change in either its bulk or surface composition.

Additional information about the identities of surface species and changes in surface compositions were obtained from the O 1*s* and C 1*s* regions in the XPS spectra of $BaPbO_3$ and $BaSnO_3$. (The behavior of $BaBiO_3$ in these spectral regions was very similar to that of $BaPbO_3$, and will not be discussed separately.) O 1*s* and C 1*s* spectra of $BaPbO_3$, following various treatments, are displayed in Figs. 6 and 7, respectively. Spectrum A in Fig. 6 was obtained with a $BaPbO_3$ sample that had been treated in flowing oxygen at 800°C for 10 h and then cooled in O_2 to room temperature. This sample had a slight (~10%) stoichiometric excess of barium, which existed as BaO_2 after the oxygen treatment, and was used in order to demonstrate the thermal behavior and O 1*s* lines of BaO_2. An XRD spectrum of this sample, following treatment in O_2 at 800°C, indicated the presence of both the $BaPbO_3$ perovskite phase and a small amount of bulk BaO_2. The C 1*s* spectrum of this material, shown in Fig. 7A, indicated that the sample contained only adventitious carbon, represented by the peak at 284.6 eV, and was free of surface carbonate species, which would have produced an additional C 1*s* peak at 288–289 eV. The O 1*s* spectrum of this sample may be deconvoluted into three distinct features. The highest intensity peak, occurring at the lowest binding energy (528.7 eV), is assigned to O^{2-} of the $BaPbO_3$ phase. The other two peaks (at 530.8 eV and 532.1 eV) are assigned to the O_2^{2-} species in BaO_2 and $BaPbO_3$, respectively. The basis for these peak assignments will be further discussed below.

The spectrum in Fig. 6B was obtained after the sample in Fig. 6A had been subsequently evacuated for 1 h at 600°C. Only two

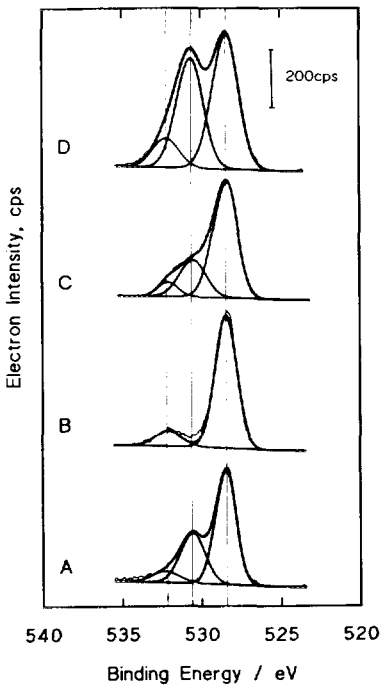

FIG. 6. XPS spectra in O 1*s* region of $BaPbO_3$. (A) after O_2 treatment at 800°C; (B) sample A after subsequent evacuation at 600°C; (C) sample B after subsequent exposure to O_2 at 500°C; (D) fresh sample after pretreatment in O_2 at 800°C and subsequent exposure to CH_4/O_2/He reaction mixture for 10 h at 800°C.

distinct features remained, having binding energies of 528.7 eV and 532.1 eV, and assigned to the O^{2-} and the O_2^{2-}, respectively, of $BaPbO_3$. (Following similar treatment in O_2 at 800°C and subsequent evacuation at 600°C, a sample of *pure* $BaPbO_3$, i.e., one containing no stoichiometric excess of Ba, gave an XPS spectrum that was identical to Fig. 6B.) Hence, evacuation at 600°C was sufficient to decompose BaO_2, at least in the near-surface region of this material. When a sample of pure BaO_2 was similarly evacuated to 600°C, its single O 1*s* peak at 530.9 eV due to O_2^{2-} disappeared, and a new feature appeared at 528.5 eV, due to the O^{2-} in BaO. Thus, the peak at 528.7 eV in Fig. 6B may contain the O^{2-} signals of both $BaPbO_3$ and BaO. The C 1*s* spectrum of this sample (Fig. 7B) again shows the presence of only adventitious surface carbon. Subsequent exposure of the sample to oxygen at 500°C (Fig. 6C) resulted in a reappearance of the feature previously observed at 530.8 eV in spectrum A, and is attributed to the reconversion of BaO into BaO_2. This conclusion is supported by the C 1*s* spectrum of this material in Fig. 7C, which again confirms that this new O 1*s* peak is not due to the formation of a surface carbonate.

The peak assignments discussed above may now be used to explain the behavior illustrated in Fig. 6D. This spectrum was obtained after exposing a sample of stoichiometric $BaPbO_3$ to the 4 : 1 CH_4/O_2 reactant mixture at 800°C for 10 h, then flowing He over the sample for another hour at the same temperature, and finally cooling in He to room temperature. (The He flush at 800°C was performed to ensure the removal of any

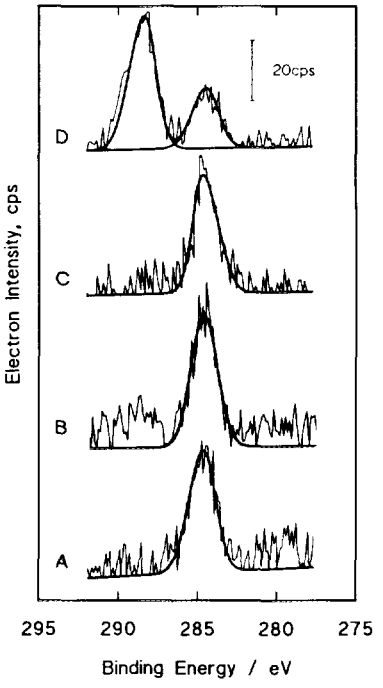

FIG. 7. XPS spectra in C 1*s* region of $BaPbO_3$. (A) after O_2 treatment at 800°C; (B) sample A after subsequent evacuation at 600°C; (C) sample B after subsequent exposure to O_2 at 500°C; (D) fresh sample after pretreatment in O_2 at 800°C and subsequent exposure to CH_4/O_2/He reaction mixture for 10 h at 800°C.

adsorbed water or surface hydroxyls, which would have contributed to the O 1*s* peak envelope and made its interpretation ambiguous. Complete removal of water and/or hydroxyls was confirmed by the deuterium exchange experiments which will be described below.) As shown in Table 2, this sample consisted primarily of $BaCO_3$ and BaO_2, as well as various lead oxides, with only about 20% of the original $BaPbO_3$ remaining in the bulk. Consistent with these XRD results, the O 1*s* spectrum in Fig. 6D may be deconvoluted into the following three features: a peak at 528.7 eV, due to O^{2-} of $BaPbO_3$, a single unresolved peak at 530.9 eV, containing the overlapping contributions from both O_2^{2-} of BaO_2 and CO_3^{2-} of $BaCO_3$, and a peak at 532.1 eV, due to O_2^{2-} of $BaPbO_3$. The presence of CO_3^{2-} in this sample is confirmed by the peak at 288.7 eV in its C 1*s* spectrum, shown in Fig. 7D. The XPS spectrum of a sample of pure $BaCO_3$ contained a single O 1*s* peak at 530.7 eV and a C 1*s* peak at 288.9 eV, the relative areas of which corresponded to a corrected O : C surface composition ratio of 3.2, which is close to the expected value of 3.0 for the pure carbonate. By contrast, the areas of the O 1*s* peak at 530.9 eV and the C 1*s* peak at 288.7 eV shown in Figs. 6D and 7D for the used $BaPbO_3$ sample correspond to an O : C surface composition ratio of 3.9, indicating that 15–20% of this O 1*s* peak is due to O_2^{2-} of BaO_2, with the remainder due to CO_3^{2-} of $BaCO_3$. Further support for these assignments was obtained from a separate experiment, in which a similarly treated sample of $BaPbO_3$ was cooled in O_2, rather than in He, following exposure to the CH_4/O_2 reaction mixture. The resulting O 1*s* spectrum was identical to that in Fig. 6D, except that the relative intensity of the peak at 530.9 eV was ~35% larger, and the calculated O : C surface composition ratio was 4.3. Thus, cooling the used sample in O_2 resulted in additional formation of BaO_2, in agreement with the behavior observed in Fig. 6C. $BaCO_3$ itself may be ruled out as the active phase, since the pure carbonate exhibits very low *initial* activity, which subsequently increases with time as the active BaO_2 phase is generated by partial decomposition of the carbonate.

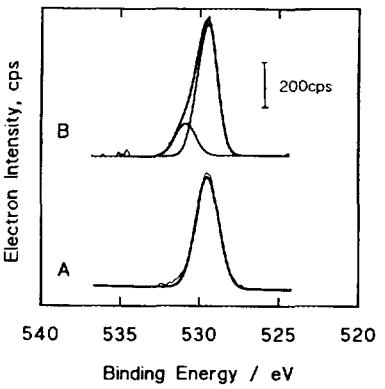

FIG. 8. XPS spectra in O 1*s* region of $BaSnO_3$. (A) after O_2 treatment at 800°C; (B) after subsequent exposure to CH_4/O_2/He reaction mixture for 10 h at 800°C.

In marked contrast to the behavior observed for $BaPbO_3$, $BaSnO_3$, when identically treated, did not undergo such complex changes in surface composition, as illustrated in Figs. 8 and 9. The O 1*s* spectrum of fresh $BaSnO_3$, after treatment in oxygen at 800°C, contained only the expected single feature at 529.2 eV, which is assigned to the O^{2-} of $BaSnO_3$. After exposure to the CH_4/O_2 reaction mixture for 10 h at 800°C,

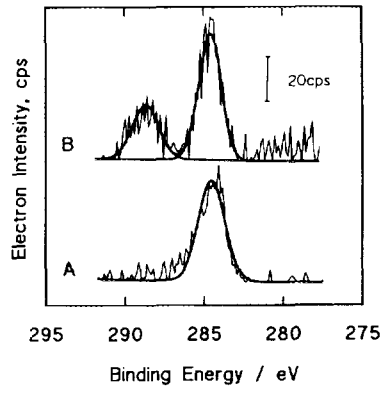

FIG. 9. XPS spectra in C 1*s* region of $BaSnO_3$. (A) after O_2 treatment at 800°C; (B) after subsequent exposure to CH_4/O_2/He reaction mixture for 10 h at 800°C.

a small amount of surface carbonate species was formed, as evidenced by appearance of the O 1*s* peak at 531.2 eV and the C 1*s* peak at 288.6 eV. The amount of the carbonate formed was evidently sufficiently small that it could not be detected by XRD analysis (Table 2), suggesting that its formation may have been limited only to the surface of this material. With $BaPbO_3$ and $BaBiO_3$, on the other hand, it appears that carbonate formation caused extensive bulk, as well as surface, transformation.

The absence of surface hydroxyls and adsorbed water, which could have contributed to the O 1*s* envelopes in Fig. 6, was confirmed by deuterium exchange experiments. Following each of the treatments described for the samples in Fig. 6, identically treated separate samples of $BaPbO_3$ were exposed at 600°C to a measured excess of D_2 in a closed reactor of accurately known volume. Samples of the gas phase were periodically analyzed by mass spectrometry. Following appropriate calibration for differing sensitivities, the equilibrated amounts of H_2 and HD observed were then used to calculate the total OH and/or H_2O content of the original catalyst sample. The accuracy and sensitivity of the technique were verified by applying it to a sample of H-Y zeolite which had been evacuated for 16 h at 400°C and then exposed to D_2 for 2 h at the same temperature. The amount of H determined for this sample by the D_2 exchange method was within 10% of the stoichiometrically expected value. For a sample of $BaPbO_3$ that had been intentionally exposed to the atmosphere, then evacuated at room temperature and exposed to D_2 at 600°C, the amount of surface OH determined by this method corresponded to 1.0 ± 0.1 monolayer, with an estimated limit of detection of ~0.01 monolayer. However, for each of the $BaPbO_3$ samples treated similarly to those shown in Fig. 6, no H_2 or HD could be detected following equilibration with D_2 at 600°C. Hence, we conclude that the residual content of hydroxyls or surface water in these samples was <1% of a monolayer, and would not have contributed measurably to the O 1*s* spectra in Fig. 6.

XPS spectra of the oxygen species in $BaPbO_3$ and $BaBiO_3$ have been reported by several previous researchers (*11–14*). The binding energies of peroxide species (O_2^{2-}) reported by Ganguly and Hegde (*12*) for $BaPbO_3$ (532.5 eV) and $BaBiO_3$ (532.4 eV) are slightly higher than those obtained in the present study (532.1 eV and 531.8 eV, respectively). Their reported binding energies of O^{2-} species (529.6 eV for $BaPbO_3$ and 529.3 eV for $BaBiO_3$) are also about 1 eV higher than the values we observed in this study (528.7 eV and 528.6 eV). Nevertheless, although the absolute binding energies reported by Ganguly and Hegde are higher than ours for both O^{2-} and for O_2^{2-}, the *difference* in binding energy between these two species was similar (2.9 to 3.3 eV) in both studies. The binding energies that we observed for the O_2^{2-} of BaO_2 formed on $BaPbO_3$ (530.8 eV) and on $BaBiO_3$ (530.6 eV), however, are about 2.0 eV lower than that reported for pure BaO_2 (533 eV) by Ganguly and Hegde. In a separate study, to be more fully described in a future paper, we have observed that BaO_2 deposited on MgO exhibits an O 1*s* binding energy of 530.9 eV, which is also 2.1 eV lower than the value reported for BaO_2 by Ganguly and Hegde. An O 1*s* binding energy of 531.0 eV for BaO_2 has been reported by Yamashita *et al.* (*10*), which closely agrees with our results.

In a previous study of $BaPbO_3$, Lunsford and Kharas (*13*) reported a significantly lower binding energy (530.1 eV) for the peroxidic oxygen in $BaPbO_3$. This value is about 2.0 eV lower than that reported in the present study and 2.6 eV lower than the binding energy of peroxidic oxygen in $BaPbO_3$ reported by Ganguly and Hegde. Furthermore, the difference in binding energies between O^{2-} (528.4 eV) and O_2^{2-} (530.1 eV) of $BaPbO_3$ reported by Lunsford and Kharas was only 1.7 eV, which is very close to the difference in binding energy between the O_2^{2-} in BaO_2 formed on $BaPbO_3$ and the O^{2-} species of the $BaPbO_3$ phase. We have

observed in the present study that the presence of excess Ba on the catalyst surfaces results in the formation of a surface BaO_2 phase upon treatment in O_2 at high temperatures. This BaO_2 could mask the O 1*s* signal of the perovskite phase, resulting in erroneous binding energies. Therefore, the discrepancy between the previous study of $BaPbO_3$, $BaBiO_3$, and $BaSnO_3$ by Lunsford and Kharas (*13, 14*) and the present study could be due to the presence of either surface OH or BaO_2 in their samples. If present, either could be misidentified as the O_2^{2-} of the perovskite phase.

The observed decompositions of the bulk perovskite phases in the Ba-Pb and Ba-Bi catalysts were accompanied by increases in intensity of the O 1*s* feature due to BaO_2 and by parallel increases in the catalytic activities of these materials for methane coupling during the first few hours of reaction. The decomposition of the perovskite phase was rapid and extensive in the case of $BaPbO_3$, slow and less extensive in the case of $BaBiO_3$, and did not occur at all with $BaSnO_3$, whose catalytic activity and selectivity did not vary with time (Fig. 1). It should also be noted that the initial increases in catalytic activity observed for $BaPbO_3$ and $BaBiO_3$ during the first two hours of reaction are smaller when the original catalysts contained excess Ba (Fig. 1). This is because the catalyst surfaces are already extensively covered with the active BaO_2 phase. In the case of $BaPbO_3$, the initial increase in activity is accompanied by a corresponding increase in C_2 selectivity as the BaO_2 phase increases, while over $BaBiO_3$, the C_2 selectivity declined slightly with time. Since these catalysts are capable of absorbing CO_2, their true initial selectivities are often masked. However, the slow decomposition of the $BaBiO_3$ phase, its somewhat lower surface area and lower methane conversion, and the saturation of the catalyst by CO_2 may result in the observed slight decrease in C_2 selectivity over this material. The initial decrease in activity of the $BaSnO_3$ catalyst containing excess Ba is due to the fact that this perovskite does not decompose under reaction conditions to produce additional BaO_2. Hence, its content of the active surface BaO_2 phase is highest at the beginning of the reaction, and it immediately begins to undergo some loss of activity due to CO_2 poisoning.

CONCLUSIONS

The perovskites $BaPbO_3$, $BaBiO_3$, and $BaSnO_3$, containing excess Ba, showed higher C_2 selectivity during methane oxidation at 800°C than did their stoichiometric counterparts. The catalytic activities of the Ba–Pb and Ba–Bi materials increased during the first 2 h of reaction, due to the partial decomposition of the stoichiometric perovskites into the more active BaO_2 phase. This increase was less pronounced in the cases where the catalysts contained an initial excess of Ba. XPS characterization of the catalysts confirmed that the surface Ba concentration increased initially and reached a steady state after about 2 h of reaction. With $BaSnO_3$, by contrast, no increase in surface Ba content was observed during reaction, and the C_2 selectivity of this material was much lower than those of the Ba–Pb and Ba–Bi perovskites. XRD analyses indicated that the excess Ba may initially exist as $BaCO_3$, which is gradually converted into BaO_2 when exposed to O_2 at high temperature. After extended (20 h) exposure to the reaction mixture at 800°C, the original bulk perovskite phases of $BaPbO_3$ and $BaBiO_3$ decreased, and BaO_2, $BaCO_3$, PbO_x, and Bi_2O_3 were formed. $BaSnO_3$ did not undergo observable changes in its bulk composition during reaction. Since the decompositions of $BaPbO_3$ and $BaBiO_3$ have no adverse effect on their catalytic activities or C_2 selectivities, the original perovskite phases of these materials may be less important in determining activity and C_2 selectivity during the oxidative coupling of methane than is the BaO_2 phase that is formed via the decomposition of the perovskite phase or by the addition of excess Ba. A significant portion of the Ba species on the surfaces of

these materials during reaction exists as $BaCO_3$, which is generated from the CO_2 reaction product and which may be partially converted into BaO_2 upon reaction with O_2 at the temperatures where the catalysts are active. Yamashita *et al.* recently reported that BaO_2 supported on La_2O_3 is reasonably active for the oxidative coupling of methane (*10*). We conclude that the active phase of $BaPbO_3$ and $BaBiO_3$ perovskites for oxidative coupling of methane is BaO_2, generated by the decomposition of the original perovskite phases.

ACKNOWLEDGMENT

The authors gratefully acknowledge financial support of this research by the National Science Foundation under Grant CHE-9005808.

REFERENCES

1. Lee, J. S., and Oyama, S. T., *Catal. Rev. Sci. Eng.* **30,** 249 (1988).
2. Scurrell, M. S., *Appl. Catal.* **32,** 1 (1987).
3. Jones, C. A., Leonard, J. J., and Sofranko, J. A., *Energy Fuels* **1,** 12 (1987).
4. Ito, T., and Lunsford, J. H., *Nature* **314,** 721 (1985).
5. Otsuka, K., Jinno, Y., Wada, Y., and Said, A. A., *J. Catal.* **121,** 122 (1990).
6. Otsuka, K., Said, A. A., Jinno, K., and Komatsu, T., *Chem. Lett.*, 77 (1987).
7. Otsuka, K., and Jinno, K., *Inorg. Chim. Acta* **121,** 237 (1986).
8. Peng, X. D., Richards, D. A., and Stair, P. C., *J. Catal.* **121,** 99 (1990).
9. Peng, X. D., and Stair, P. C., *J. Catal.* **128,** 264 (1991).
10. Yamashita, H., Machida, Y., and Tomita, A., *Appl. Catal. A: General* **79,** 203 (1991).
11. Rao, C. N. R., Ganguly, P., and Sarma, D. D., *J. Am. Chem. Soc.* **109,** 6893 (1987).
12. Ganguly, P., and Hegde, M. S., *Phys. Rev. B.* **37,** 5107 (1988).
13. Kharas, K. C. C., and Lunsford, J. H., *J. Am. Chem. Soc.* **111,** 2336 (1989).
14. Kharas, K. C. C., and Lunsford, J. H., *Prepr. Am. Chem. Soc. Div. Petr. Chem.* **35,** 200 (1990).
15. Vidyasagar, K., Gopalakrishnan, J., and Rao, C. N. R., *J. Solid State Chem.* **58,** 29 (1985).